

Earth Sensing in the Dolomites: A Summer School for Capacity Building and Collaboration on Geomatics for Environmental Applications

Larissa Maria Granja^{1,2}; Erico Kutchartt^{1,3}; Enrico Magazzino^{1,2}; Thomas Zieher⁴; Rasoul Eskandari⁵; Michele Crosetto⁶; Caterina Balletti⁷; Andrea Martino⁷; Mattia Balestra^{8,9}; Roberto Pierdicca⁹; Lindo Nepi¹⁰; Carlos Cabo¹¹; Anna Iglseder¹²; Mauricio Acuna¹³; Borja García Pascual^{13,14}; Francesco Pirotti^{1,2}

¹ Department of Land, Environment, Agriculture and Forestry (TESAF), University of Padova, Viale dell'Università 16, Legnaro, PD 35020, Italy – (larissamaria.cavalcantefalcao@unipd.it, erico.kutchartt, francesco.pirotti)@unipd.it

² Interdepartmental Research Center of Geomatics (CIRGEO), University of Padova, Corte Benedettina, Via Roma 34, Legnaro, PD 35020, Italy

³ Forest Science and Technology Centre of Catalonia (CTFC), Carretera de Sant Llorenç de Morunys, Km 2, 25280 Solsona, Spain – erico.kutchartt@ctfc.cat

⁴ Department of Natural Hazards, Austrian Research Centre for Forests (BFW), Rennweg 1, 6020 Innsbruck, Austria – thomas.zieher@bfw.gv.at

⁵ Department of Architecture, Built Environment and Construction Engineering, Politecnico di Milano, via Ponzio 31, 20133 Milano, Italy – rasoul.eskandari@polimi.it

⁶ Centre Tecnològic de Telecomunicacions de Catalunya (CTTC/CERCA), Geomatics Division, Av. Gauss, 7, E-08860 Castelldefels (Barcelona), Spain – mcrosetto@cttc.cat

⁷ Università Iuav di Venezia, Santa Croce, 191, Venezia, VE 30135, Italy – (caterina.balletti, amartino)@iuav.it

⁸ Department of Agricultural, Food and Environmental Sciences (D3A), Università Politecnica delle Marche, Ancona, 60131, Italy – m.balestra@staff.univpm.it

⁹ Department of Civil, Building and Architectural Engineering (DICEA), Università Politecnica delle Marche, Ancona, 60131, Italy – r.pierdicca@staff.univpm.it

¹⁰ Department of Information Engineering (DII), Università Politecnica delle Marche, Ancona, Italy – l.nepi@pm.univpm.it

¹¹ Department of Mining Exploitation and Prospecting, University of Oviedo, Campus de Mieres, 33600 Mieres, Oviedo, Spain – carloscabo@uniovi.es

¹² Department of Geodesy and Geoinformation, TU Wien, Wiedner Hauptstraße 8-10, 1040 Vienna, Austria – anna.iglseder@geo.tuwien.ac.at

¹³ Forest Technology and Wood Material Solutions, Natural Resources Institute Finland (Luke), 80100 Joensuu, Finland – (mauricio.acuna, borja.garcia.pascual)@luke.fi

¹⁴ School of Forest Sciences, University of Eastern Finland, 80101 Joensuu, Finland – borja.garcia.pascual@uef.fi

Keywords: interdisciplinary training, sensing technologies, terrestrial laser scanner, mobile laser scanner, unmanned aerial vehicle, synthetic aperture radar

Abstract

Capacity building is a key element in promoting and training in spatial technologies and in fostering a network of early-stage researchers for future collaborations. The first edition of the Earth Sensing Summer School, organised by the University of Padova with support from ISPRS Education and Capacity Building (ECBI) funds, was held from 7 to 13 September 2025 in the Dolomite area of the Alpine region. This article illustrates specific aspects of the organisation and discusses the return on investment in terms of training and networking. It highlights the methodology used for selecting participants and conducting the training, which included a balanced combination of seminars, fieldwork, data analysis, dissemination to peers, and a final defence of results. We discuss the outcomes and feedback from the almost 40 participants and provide ideas for future improvements, aiming to offer insights for fellow researchers who might want to replicate a capacity-building activity of this kind.

1. Introduction

Training activities represent a fundamental component of scientific research. They not only ensure the transfer of knowledge across generations of researchers but also foster enduring professional networks among participants. Various approaches can be adopted in teaching and training, and summer schools are particularly distinctive in bringing together a selected group of participants and supervisors around a common scientific theme. Summer schools may differ in structure and objectives; in this context, the term refers to intensive week-long programmes focused on specific topics, combining theoretical lectures with practical sessions. The Earth Sensing Summer School format originated from another ISPRS-supported Summer School, "Sensing Mountains" organised by the University of Innsbruck, which is now reaching its sixth edition (Rutzinger et al., 2016, 2018, 2020). As a biennial event centred in a mountain area, the

Earth Sensing Summer School alternates with Sensing Mountains, taking place in the intervening years. In this way, the two initiatives jointly provide an annual training opportunity for the scientific community. A distinctive feature of these events is that all activities are concentrated at a single location, minimising the need for participants to leave the premises except for field data collection. This setting fosters continuous interaction among participants and instructors, enhancing both collaborative work and informal exchanges throughout the event.

2. Materials and methods

2.1 Study area

The summer school took place in the Dolomites (Eastern Italian Alps), in the municipality of San Vito di Cadore (Province of Belluno) (Figure 1). Located at approximately 1,010 m a.s.l. San

Vito lies at the foot of two Dolomite peaks, Mount Antelao (3,264 m) and Mount Pelmo (3,168 m). The climate is alpine, with long, snowy winters and cool summers. Precipitation is strongly influenced by orographic effects, as moist air is forced over steep mountain slopes, producing high annual rainfall. In summer, short but very intense convective storms occur, characterised by heavy rainfalls in a short time. The area is characterised by formations such as the Dolomia Principale and Calcarei Grigi. These formations are heavily fractured, and during intense rainfall, the resulting loose material can be mobilised into debris flows, making these geological formations an important factor in local slope instability and natural hazards. Such processes have been the subject of extensive hydrological and geomorphological research in the region.



Figure 1. Earth Sensing Summer School Location. Municipality of San Vito di Cadore, Italy.

Coniferous forests of *Picea abies* and *Larix decidua* dominate the vegetation, and forest ecosystems are shaped by natural disturbances and centuries of human use (Rogora et al., 2018). The interplay of geology and landscape has led the Dolomites to be designated a UNESCO World Heritage Site. Its strategic location and environmental diversity make San Vito di Cadore a suitable "open-air laboratory" for educational activities such as the Earth Sensing Summer School, which offers participants direct experience with alpine ecosystems and natural hazards.

2.2 Enrollment

Applications were evaluated on merit through an online form requiring a CV, motivation letter, and extended abstract of previous work. A selection committee ranked and shortlisted eligible candidates, ensuring gender balance, and invited the first forty to participate.

2.3 Keynotes

The following keynote speakers supported our summer school by providing seminars with the following titles: "Photogrammetry and Nerf/Gaussian Splats in Forest Environments" by Mauricio Acuna (LUKE - Finland); "Geomatics for Environmental Management" by Nicholas Coops (University of British Columbia - Canada); "Terrestrial photogrammetric techniques for glacier monitoring at high spatial and temporal resolution" by Hans-Gerd Maas (Technical University Dresden - Germany); "Deformation monitoring using interferometric SAR and the

European Ground Motion Service" by Michele Crosetto (CTTC - Spain); "Active remote sensing for environmental applications" by José Manuel Delgado Blasco (ESA Φ-lab - Italy); "Single-tree based forest assessment and monitoring" by Xinlian Liang (Wuhan University - China); and "Integration of multisensor remote sensing for mapping and modelling trees and forests" by Gherardo Chirici (University of Florence - Italy - IUFRO).

2.4 Objectives and team assignments

The Earth Sensing Summer School aimed to bring together early-stage researchers in geomatics, spatial science, and remote sensing, with a focus on environmental applications. Six group assignments, each supervised by two scientists, addressed different aspects of sensing technologies. The following sections describe each assignment, summarising their objectives, design, and main outputs. Data collection relied on task-specific sensors, which were presented to all participants during a dedicated half-day demonstration session (Figure 2).

2.4.1 Assignment A - The Battle of the Beams: focused on assessing forest structure using different LiDAR sensors and platforms. Activities took place in a mixed coniferous stand, using Terrestrial (TLS), Mobile (MLS), and UAV Laser Scanning (ULS) over a 2,500 m² forest plot representative of the area. The objective was to introduce students to state-of-the-art proximal sensing and point cloud processing in forest environments, highlighting the strengths and limitations of different sensors. These methods were linked to broader forest functions, such as economic, ecological, protective, and recreational, guiding students to formulate their own research questions for data analysis.



Figure 2. MicaSense Altum PT (A), Stonex x120go SLAM (B), Riegl VZ600-i (C) and SILVA Rover by CISAS (D).

Participants designed and carried out a complete data acquisition campaign, including 21 TLS scans, MLS surveys with two handheld systems, and a 30-minute ULS flight. Data analysis focused on comparing sensor accuracy and coverage, deriving forest structural parameters (e.g., stem density and canopy gap fraction), and producing a sapling suitability map based on terrain and canopy characteristics. Point clouds were first processed with

manufacturer software and aligned in CloudCompare; stem metrics were extracted using the 3DFin plugin (Laino et al., 2024), while ArcGIS Pro and WhiteboxTools were used to generate DEMs and terrain derivatives. A canopy height model derived from ULS and complemented by MLS and TLS data supported canopy openness analysis. By integrating slope, canopy gaps, and obstacles, a sapling suitability index at 50 cm resolution was computed and validated against manually identified saplings. Results highlighted complementary strengths of the platforms: TLS provided the highest geometric accuracy and understory detail, ULS ensured superior canopy coverage, and MLS enabled rapid data collection. The sapling suitability analysis, visualised in Figure 3, demonstrated that combining topographic and canopy variables derived from LiDAR data can effectively identify microhabitats favourable for regeneration and provide a useful application for LiDAR point clouds in forest environments. Overall, the exercise offered hands-on experience across the full LiDAR workflow and encouraged critical reflection on trade-offs between accuracy, coverage, and efficiency, demonstrating the value of multi-sensor approaches for forest monitoring and management.

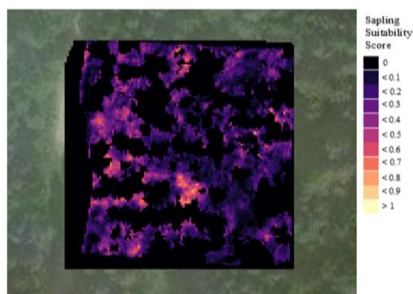


Figure 3. Sampling suitability score, based on ground obstacle layer, slope, topographic depression and canopy density.

2.4.2 Assignment B - Ground movement from RADAR InSAR Challenge: aimed to familiarise participants with radar interferometry techniques for ground motion analysis and landslide monitoring. Using SARAXIO[®], a newly developed InSAR processing software, the group generated and analysed deformation time series from Sentinel-1 data over the southern slope of Mount Antelao (San Vito di Cadore, Italy), an area affected by active landslides. To assess SARAXIO[®]'s performance and reliability, the outputs were compared with validated products from the European Ground Motion Service (EGMS) (Figure 4). Participants processed Sentinel-1 SAR images from a descending orbit track, following the main steps of InSAR workflows, including co-registration, interferogram generation, phase unwrapping, and multi-temporal analysis, while testing the influence of several parameters, including velocity models, coherence and amplitude dispersion thresholds, and the selection of Persistent Scatterers (PS) and Distributed Scatterers (DS).

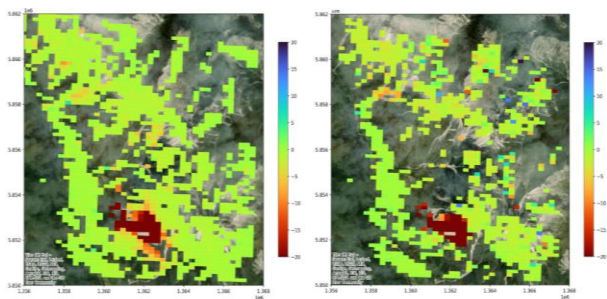


Figure 4. Zoom of the processed area showing deformation velocity from EGMS data (right) and SARAXIO data (left).

By adjusting these parameters, they explored how different processing choices affect the detection and characterisation of slope instabilities. The analysis showed that a linear velocity model provided the best agreement with the EGMS time series, while higher-order models reduced coherence and the number of valid measurement points. Including DS resulted in marginal improvements but could also introduce noise under suboptimal conditions. Overall, SARAXIO[®] successfully reproduced the main deformation patterns observed by EGMS, with inconsistencies mainly related to atmospheric corrections and geocoding. Beyond the technical results, the exercise offered participants a comprehensive, hands-on experience with radar data processing and critical evaluation of algorithmic choices. It highlighted the practical challenges associated with InSAR analysis in mountainous terrain and strengthened participants' understanding of how methodological parameters influence data quality and interpretation.

2.4.3 Assignment C - Urban 3D Modelling Challenge: participants designed and executed an end-to-end workflow to integrate mobile laser scanning (MLS) with UAV surveys for the alpine town centre. The group planned overlap-rich SLAM scans along streets and tight corridors and complementary UAV flights to capture rooftops, open surfaces, and the broader urban morphology, aiming to produce a unified 3D dataset suitable for accessibility-oriented analysis (e.g., slopes, bottlenecks, architectural barriers). The acquisition combined SLAM-based MLS (STONEX X120GO; XGRIDS Lixel L2 Pro) for dense close-range geometry with UAV platforms (DJI Mavic 3 Multispectral; DJI Matrice 350 RTK with LiDAR) to extend coverage and volumetric detail. Processing followed sensor-specific pipelines: GOpst and LixelStudio for SLAM drift mitigation and georeferencing; DJI Terra for UAV LiDAR trajectory refinement and point-cloud generation; and Agisoft Metashape for Structure-from-Motion on RGB/multispectral imagery. In addition, before classification and merging in LiDAR360, cross-sensor comparisons were performed in CloudCompare, with final compilation completed in Agisoft Metashape. Deliverables included an orthomosaic at 10 cm/pixel, a DTM, a DSM, and a merged point cloud that supported slope mapping and preliminary clearance analysis across the town centre. Cross-sensor checks showed coherent urban geometry in overlapping areas, while fusion improved completeness. UAV data efficiently covered roofs and wide planar surfaces with relatively homogeneous, lower point densities. In contrast, MLS achieved much higher local densities at street level, enabling detection of obstacles and small-scale discontinuities relevant to accessibility (Figure 5).

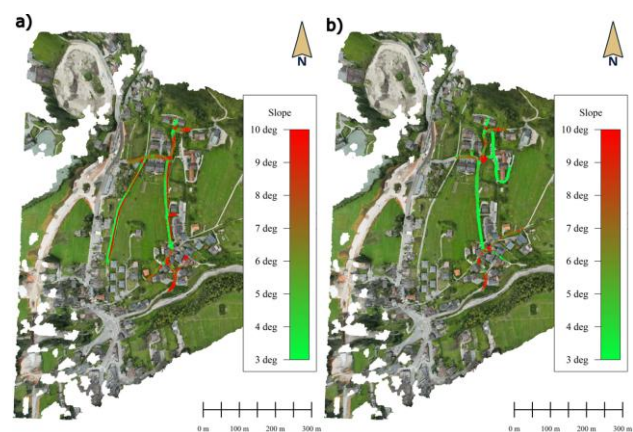


Figure 5. Road slope analysis for a) Stonex X120GO and b) Lixel L2Pro.

Educationally, the assignment emphasised method selection (deciding when to favour aerial coverage versus ground-level detail), practical data-quality awareness (e.g., SLAM drift, registration consistency), and collaborative workflow management mirroring professional roles from flight planning to GIS analysis. The group also documented operational and methodological challenges typical of mountainous urban settings, such as weather and regulatory constraints for UAVs, line-of-sight issues, SLAM drift, and the demands of harmonising heterogeneous point clouds. The participants also proposed refinements for future editions, such as brief calibration/benchmarking exercises (e.g., TLS or GNSS control) and a lightweight "accessibility toolkit" to streamline indicator computation while preserving hands-on processing. Overall, the activity demonstrated that combining UAV photogrammetry/LiDAR with SLAM-based MLS yields a dense, spatially complete urban model that is directly useful for teaching, accessibility mapping, and planning support in alpine contexts where occlusion and topographic complexity constrain single-sensor approaches.

2.4.4 Assignment D - Remote Sensing and Environmental Modelling Challenge: the group parameterised the process-based soil–vegetation–atmosphere transfer (SVAT) model LWF-Brook90, based on the original Brook90 model (Federer et al., 2003; Schmidt-Walter et al., 2020). This enabled simulation of daily stand-level water balance for a south-facing coniferous forest near San Vito di Cadore (Belluno, Italy). The model integrated local meteorological drivers, field-measured soil properties, and forest stand structure with multi-sensor remote sensing data. Soil-horizon characteristics (texture, bulk density, organic carbon, coarse fragments) were used to construct a multilayer soil profile following the Ad-Hoc-AG Boden (2005) classification, complemented by regionally gridded pedological maps (Hengl et al., 2017). Vegetation parameters were derived from terrestrial and UAV-borne laser-scanning point clouds (individual tree height and DBH). LiDAR point clouds for the sample plot were processed in CloudCompare v2.13.12 using the 3DFin plugin v4.6.0 (Laino et al., 2024) to extract stand-structure metrics (Figure 6) suitable for model parameterisation.

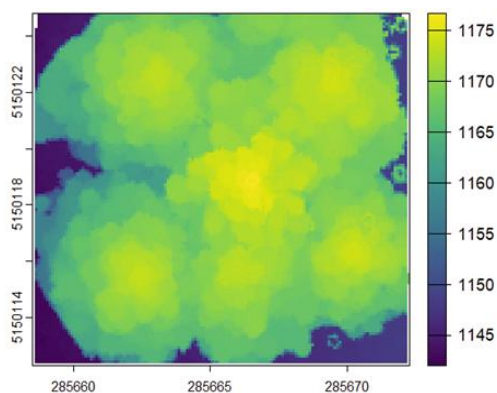


Figure 6. Tree canopy detection from UAV-LiDAR.

Indices time series based on optical satellite imagery from Sentinel-2 (NDVI, NDMI, NDWI, and MSI) were computed to assess vegetation dynamics and water stress, while Harmonised Landsat–Sentinel-2 (HLS) surface reflectance provided a temporally dense record (2–3-day global revisit) to support time-series analysis. For radar, Sentinel-1 C-band data acquired in Interferometric Wide (IW) mode (dual polarisation VV, VH) were accessed via Google Earth Engine (COPERNICUS/S1_GRD), which supplies thermally de-noised, radiometrically calibrated, and terrain-corrected backscatter

together with incidence angles. Dual-polarisation metrics (e.g., cross-ratio and RVI) were derived to screen anomalies. All preprocessing and time-series analyses (optical and SAR) were performed in Google Earth Engine, ensuring consistent compositing, cloud masking, and stack harmonisation (Drusch et al., 2012; Torres et al., 2012; Gorelick et al., 2017). Model outputs comprised water-balance components and Relative Extractable Water (REW) for 2019–2024 (Figure 7), with the 2022 northern Italy drought used as a focal test event (European Commission & Joint Research Centre, 2022).

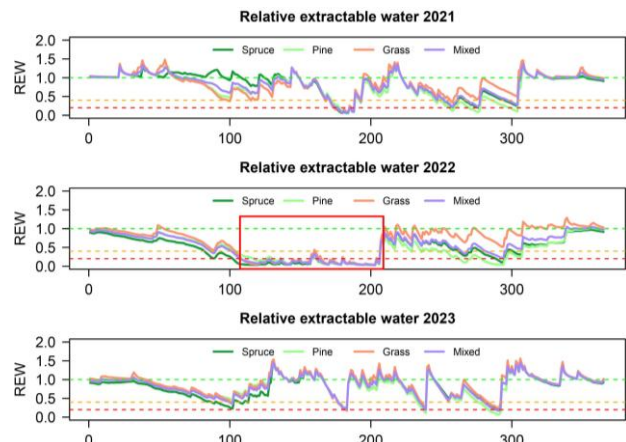


Figure 7. Relative Extractable Water (REW) 2021–2023. The red rectangle evidences the severe drought that occurred in the area in 2022.

Validation was performed using satellite and hydrometric data, with careful management of computational resources. Methodologically, the workflow follows the Brook90 lineage and recent LWF-Brook90 applications in forest hydrology and drought assessment, including comparisons with Sentinel-2–derived stress indicators and regional soil-moisture monitoring/forecasting (Meusburger et al., 2022; Vorobevskii et al., 2024a, 2024b). Overall, the results emphasise (1) the high sensitivity of LWF-Brook90 to vegetation parameterisation, (2) the practical value of harmonising soil records obtained in the field with SoilGrids, and (3) the feasibility, yet challenge, of scaling beyond the plot due to model limitations regarding lateral flows, validation constraints, and computational load (Hengl et al., 2017; Schmidt-Walter et al., 2020; Meusburger et al., 2022; Vorobevskii et al., 2024a, 2024b).

2.4.5 Assignment E - GeoAI for Environmental Analyses: the group developed an instance segmentation pipeline to identify forest, grassland, and related land-cover classes in high-resolution orthophotos using the Ultralytics YOLOv11 framework. The workflow incorporated image selection, class design, annotation and augmentation, model training, and evaluation on held-out areas. Annotations were created using Roboflow and augmented (rotations, flips, and illumination tweaks) to balance the classes. The trained network was then exported to ONNX and inspected in QGIS using the DEEPNESS/auxiliary scripts. Source imagery included Italian National and Veneto Region geoportals (0.3–0.5 m), Swiss orthophotos (0.1 m) and Google Satellite (0.1 m). A set of 650 images was tiled into 1000×1000 px chips, allocating 524 (81%) to training and 124 (19%) to validation across ten classes (forest, grassland, shrubland, cropland, rivers, roads, urban, lakes, rocky/bare, snow). Five augmented variants per labelled image were generated (horizontal flip; ±1° rotation; ~4% grayscale; ±7% saturation; ±5% exposure; ≤0.2 px blur). The final YOLOv11 run utilised 300 epochs (batch size 16, Adam, weight

decay 0.0005) and was assessed using confusion matrices and area statistics against CORINE 2020 (Figure 8). Three staged experiments illustrate learning dynamics: an initial model (547 train / 20 val) reached $mAP@0.5 \approx 34\%$; after label cleanup, a second run (1,200 / 50) improved to $\approx 45\%$; a third run (1,500 / 200) dropped to $\approx 38\%$, underscoring sensitivity to class balance and annotation consistency. Outputs were rasterised at ~ 0.3 m thematic resolution and qualitatively compared with the Veneto CLC-derived layer for San Vito di Cadore. Practical takeaways included harmonising the working legend with CLC for cleaner comparisons, reserving site-specific classes (e.g., urban parks) to limit misinterpretation with forest and extending training (beyond ~ 120 – 300 epochs) to stabilise learning where within-class variability is high (notably grasslands). Regional context for Belluno's forest expansion and land-use transitions informed label boundaries and error analysis, drawing on evidence of succession from abandoned grasslands to early woodland and related socio-ecological change (Giupponi et al., 2006; Valle et al., 2009; Painsi, 2019). The orthophoto review corroborates these transitional zones, which help explain model confusion at diffuse edges and support the ecological plausibility of the predictions.

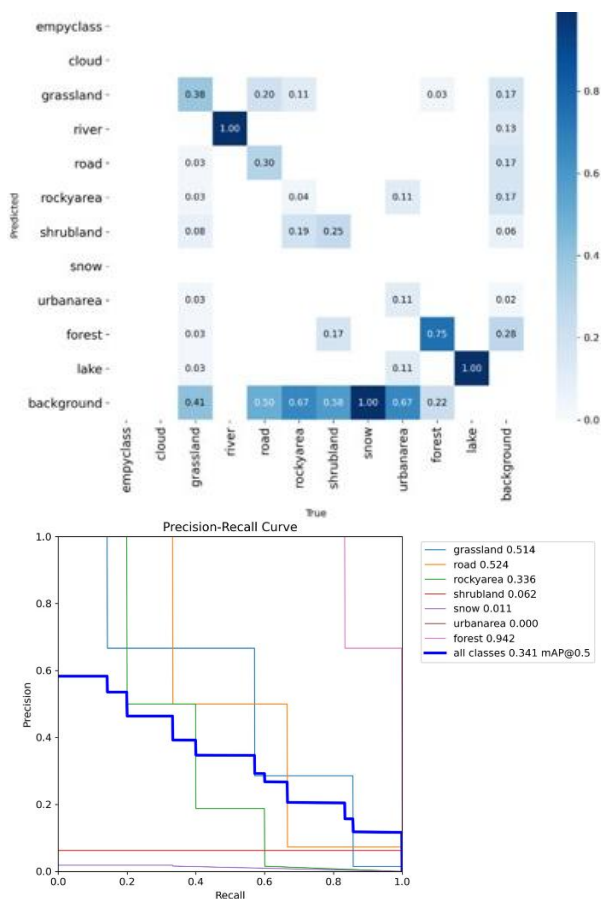


Figure 8. Confusion matrix (top) and validation accuracy curves for segmentation (bottom).

2.4.6 Assignment F – Photogrammetry and NeRF/Gaussian Splats in Forest Environments: the group compared three 3D reconstruction approaches (classical photogrammetry (SfM/MVS), Neural Radiance Fields (NeRF), and 3D Gaussian Splatting (Kerbl et al., 2023) to evaluate their usefulness for tree- and stand-level structure analysis, DBH estimation, and realistic visualisation in Alpine Forest plots near the Centro Studi per l'Ambiente Alpino in San Vito di Cadore. Field data included drone RGB and Insta360 X5 imagery, manual DBH

measurements with a calliper, and LiDAR acquired using a handheld SLAM scanner (Stonex X120GO) and an iPad Pro 2 (Polycam). These handheld/mobile LiDAR systems rapidly produced dense point clouds of stems and crowns by combining laser range measurements with real-time trajectory estimation, enabling fast plot coverage in the field (Wehr & Lohr, 1999; Vosselman & Maas, 2010). Image sets from the Insta360 X5 were processed in Agisoft Metashape using masked multi-camera inputs and high-density reconstruction settings, following established close-range photogrammetric practice in forest environments (Westoby et al., 2012; Iglhaut et al., 2019). Furthermore, the GumRoad software was used to automatically remove unwanted objects (e.g., the person carrying the camera), thereby facilitating the further processing of images captured with the Insta360 X5 camera. The resulting photogrammetric point clouds were scaled and aligned to LiDAR point clouds using RANSAC feature matching (Choi et al., 2015) and ICP registration (Chen & Medioni, 1992). These point clouds were then filtered to remove outliers, improving stem segmentation and DBH estimation. DBH was estimated using 3DFin, which isolates stems from the point cloud and fits circles around breast height for DBH extraction (Figure 9).



Figure 9. Individual trees segmented using 3DFin.

NeRF models were trained using the Nerfstudio framework with the Nerfacto method (Tancik et al., 2023), which learns a continuous radiance field mapping 3D spatial coordinates and viewing directions to colour and volumetric density, following the original NeRF formulation (Mildenhall et al., 2020). Two experimental configurations were evaluated. A tile-based run, using approximately 1,020 input frames, generated around 1,005,817 reconstructed points and required roughly four hours of processing time. In contrast, a frame-based run using a reduced input set of 67 frames produced a comparable point count (approximately 1,006,396 points) but required close to five hours to complete. Despite similar outputs densities, reconstruction quality varied and was influenced by several factors, including residual fisheye lens distortion, inconsistencies in camera pose estimation, and incomplete or weak sparse reconstructions during the structure from motion stage. In parallel, Gaussian Splatting pipelines, specifically Splatfacto and PostShot (Xu et al., 2024), were tested and demonstrate the ability to generate dense point representations and highly realistic renderings in substantially shorter processing times (Figure 10). These methods enabled near-real time visualization and interactive inspection of forest structure, making them particularly effective for qualitative analysis and communication. However, the free versions of available tools impose limitations on geometry export and downstream quantitative use (Kerbl et al., 2023). Overall, photogrammetry registered to LiDAR gave the most consistent geometric basis for DBH measurement. At the same time, NeRF and Gaussian Splatting provided visually rich reconstructions of

crowns and stand structure that are useful for communicating forest condition and canopy complexity (Kerbl et al., 2023; Tancik et al., 2023; Mildenhall et al., 2020).



Figure 10. View rendered through Gaussian splatting.

3. Results and Discussion

More than 100 applications were received, and the shortlisted candidates were distributed globally. Their characteristics are illustrated in Table 1 and Figure 11.

Below the map with affiliations of applicants.



Figure 11. Map with applicants' affiliations and locations.

Table 1. Overall country distribution of participants (F = female, M = male). Countries outside the continent where the school was held are highlighted in bold.

Country	F	M	Tot
Belgium	1		1
Brasil	1		1
Canada	1		1
China	1		1
Croatia		1	1
Finland		1	1
France		2	2
Germany	1		1
Ghana		1	1
Greece	2		2
India	1	1	2
Italy	8	5	13
Japan	2		2
Malaysia		1	1
Poland	2	4	6
Romania		1	1
Switzerland	1	1	2
TOT	21	18	39

The summer school hosted 39 participants, selected with attention to gender and origin neutrality. Moreover, 6 supervisors

and 13 speakers (welcome speeches, keynotes, and seminars). Participants represented a broad range of career stages: 4 MSc students, 9 first-year PhD candidates, 14 second-year PhD candidates, 3 third-year PhD candidates, 1 fourth-year PhD candidate, 4 post-docs, and 4 professionals (Figure 12). This distribution shows that most attendees were in the early phases of their research careers, while still including more senior researchers and professionals who could act as technical multipliers within their own institutions.

To evaluate the school and collect input for future editions, an anonymous questionnaire was distributed at the end of the program. Seventeen out of 39 participants responded (~44%). The questionnaire was organised into three main areas: 1) organisational aspects (location, facilities, and daily schedule), 2) the assignment blocks (clarity, workload, scientific value), and 3) visibility and recruitment (how participants first heard about the school. In addition, respondents were given space to provide open comments on strengths, weaknesses, and suggestions for improvement in free text.

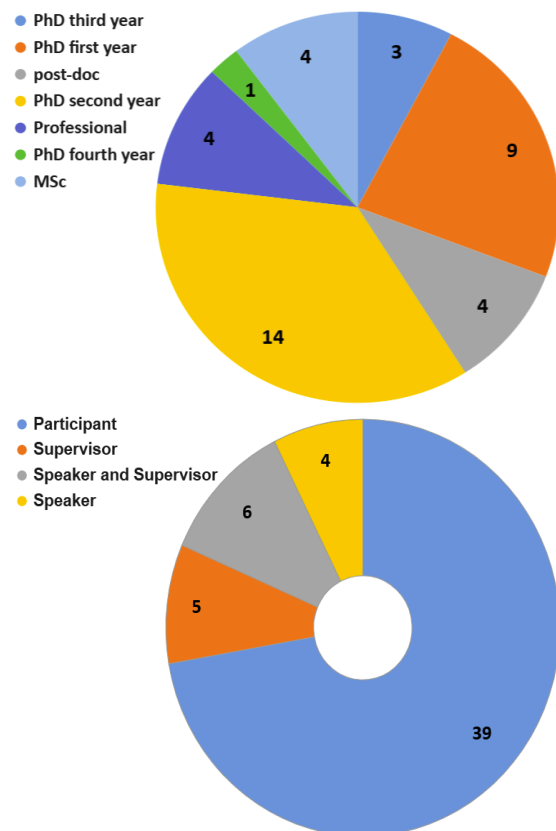


Figure 12. Participants' career stage (top); participants' role in the Summer School (bottom).

Overall satisfaction with the organisation of the school is reported in the plots in Figures 13 and 14. Figure 13, "Location", shows a median rating of 9/10 with almost no spread, indicating that participants were satisfied with the venue. "Facilities" (teaching rooms and shared work areas) show a median rating of 8/10. The balance of the daily "Schedule", the mix of lectures, field work, analysis time, and presentations also shows a median of 8/10 in Figure 13. Unlike "Location" and "Facilities," however, the "Schedule" box is wider and extends down to scores of 4/10, suggesting that while most participants found the timetable manageable, a few students experienced it as too

compressed and asked for more time for data processing, group work, and presentation preparation.

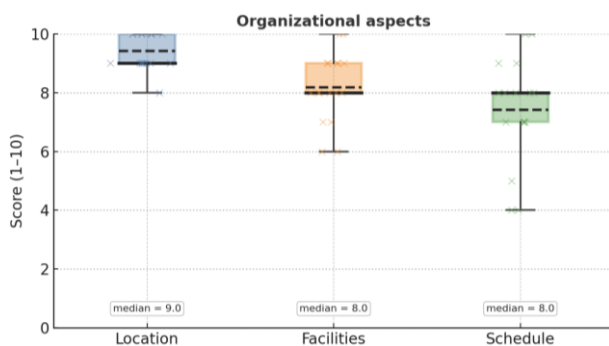


Figure 13. Organisational aspects boxplot.

The scientific training component, particularly the group assignments, was consistently highlighted as one of the summer school's strongest aspects. In Figure 14, the "Clarity" of the assignment goals shows a median of 9/10, and the perceived "Value" of the assignment for the participant's knowledge base also displayed a median of 9/10.

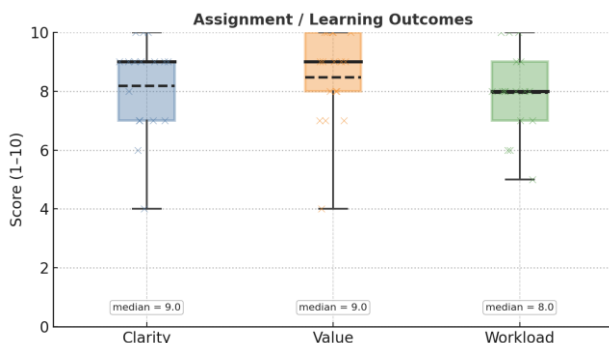


Figure 14. Assignment and Learning Outcomes Boxplot.

This confirms that the assignment model, combining hands-on data collection and analysis with expert guidance in topics such as LiDAR surveying and processing, InSAR ground motion analysis, 3D modelling, environmental/urban analysis, and GeoAI workflows are effective for skill transfer. The "Workload" boxplot shows a median of 8/10, with a few lower values, suggesting that some respondents found doing acquisition, processing, interpretation, and presentation within one week to be intense.

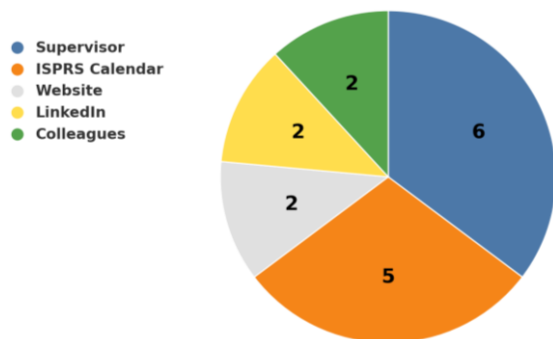


Figure 15. Pie chart of Information Sources.

This comment about workload (Figure 14) is consistent with the wider spread in the "Schedule" scores in Figure 13. In addition, the way participants first became aware of the summer school is

summarised in Figure 15. The figure shows clearly that the dominant channels were direct academic communication ("Supervisor") and discipline-specific visibility ("ISPRS Calendar"), followed by the official website, LinkedIn, and colleagues. Two points can be derived from the analysis for future editions. First, the school is already circulating through active research networks rather than relying solely on generic advertising, and second, supervisor- and institute-level communication remains the main driver to attract motivated applicants.

4. Conclusions

In this first edition of the Earth Sensing Summer School, 39 early-career participants engaged in six hands-on assignments covering forest LiDAR, InSAR ground-motion analysis, urban 3D modelling, SVAT water-balance modelling, GeoAI segmentation, and photogrammetry/NeRF-Gaussian splatting. Each group of participants produced tangible outputs and reproducible workflows. The selection process ensured international reach and balanced gender representation, while the "single-site" setup amplified peer learning and mentor interaction. Survey feedback rated location and facilities highly and confirmed the educational value of the assignment model; it also highlighted the need for slightly more time for processing, group work, and presentation preparation. Together, these results indicate a strong return on investment for capacity building and network formation and validate the alternation with the "Sensing Mountains" school to sustain an annual training cadence. By consolidating multi-sensor practice, transparent processing chains, and collaborative problem-solving in a real Alpine laboratory, the Earth Sensing Summer School offers a scalable template for training the next generation of researchers and practitioners in environmental sensing.

Acknowledgements

This work was supported by the ISPRS Education and Capacity Building Initiatives 2024, the Italian Society of Photogrammetry and Surveying (SIFET), the Shaping a World Class University program at University of Padova, the 3dForEcoTech COST Action CA20118, and by the EU MSCA Staff exchange DecisionES (grant agreement N°101007950). Larissa Granja was supported by the European Union NextGenerationEU funding. Dr. Erico Kutchartt was supported by Fondazione Cassa di Risparmio di Padova e Rovigo (CARIPARO). In-kind and promotion support was provided by: IUFRO International Union of Forest Research Organizations, CISAS Centro di Ateneo di Studi e Attività Spaziali "Giuseppe Colombo" University of Padova, with the E-FORESTER MSCA Staff Exchange Project (HORIZON-MSCA-2023-SE-01-01 — Project 101182985); the ISPRS Student Consortium, and the Società Italiana di Selvicoltura ed Ecologia Forestale (SISEF).

References

Ad-hoc-AG Boden. (2005). *Bodenkundliche Kartieranleitung* (5th ed.). Federal Institute for Geosciences and Natural Resources.

Chen, Y., & Medioni, G. (1992). Object modelling by registration of multiple range images. *Image and vision computing*, 10(3), 145-155.

Choi, S., Zhou, Q. Y., & Koltun, V. (2015). Robust reconstruction of indoor scenes. In *Proceedings of the IEEE conference on computer vision and pattern recognition* (pp. 5556-5565).

- Drusch, M., Del Bello, U., Carlier, S., Colin, O., Fernandez, V., Gascon, F., Hoersch, B., Isola, C., Laberinti, P., Martimort, P., Meygret, A., Spoto, F., Sy, O., Marchese, F., & Bargellini, P. (2012). Sentinel-2: ESA's optical high-resolution mission for GMES operational services. *Remote Sensing of Environment*, 120, 25–36.
- European Commission, & Joint Research Centre. (2022). *Drought in Northern Italy March 2022 – GDO analytical report*. Publications Office of the European Union.
- Federer, C. A., Vörösmarty, C., & Fekete, B. (2003). Sensitivity of annual evaporation to soil and root properties in two models of contrasting complexity. *Journal of Hydrometeorology*, 4(6), 1276–1290.
- Giupponi, C., Ramanzin, M., Sturaro, E., & Fuser, S. (2006). Climate and land use changes, biodiversity and agri-environmental measures in the Belluno province, Italy. *Environmental Science & Policy*, 9, 163–173.
- Gorelick, N., Hancher, M., Dixon, M., Ilyushchenko, S., Thau, D., & Moore, R. (2017). Google Earth Engine: Planetary-scale geospatial analysis for everyone. *Remote Sensing of Environment*, 202, 18–27.
- Hengl, T., Mendes de Jesus, J., Heuvelink, G. B. M., Ruiperez Gonzalez, M., Kilibarda, M., Blagotić, A., Shangguan, W., Wright, M. N., Geng, X., Bauer-Marschallinger, B., Guevara, M. A., Vargas, R., MacMillan, R. A., Batjes, N. H., Leenaars, J. G. B., Ribeiro, E., Wheeler, I., Mantel, S., & Kempen, B. (2017). SoilGrids250m: Global gridded soil information based on machine learning. *PLOS ONE*, 12(2), e0169748.
- Iglhaut, J., Cabo, C., Puliti, S., Piermattei, L., O'Connor, J., & Rosette, J. (2019). Structure from motion photogrammetry in forestry: A review. *Current Forestry Reports*, 5(3), 155–168.
- Kerbl, B., Kopanas, G., Leimkühler, T., & Drettakis, G. (2023). 3D Gaussian splatting for real-time radiance field rendering. *arXiv preprint arXiv:2308.04079*.
- Laino, D., Cabo, C., Prendes, C., Janvier, R., Ordonez, C., Nikonovas, T., Doerr, S., & Santin, C. (2024). 3DFin: A software for automated 3D forest inventories from terrestrial point clouds. *Forestry: An International Journal of Forest Research*, 97(4), 479–496.
- Meusbürger, K., Trotsiuk, V., Schmidt-Walter, P., Baltensweiler, A., Brun, P., Bernhard, F., Gharun, M., Habel, R., Hagedorn, F., Köchli, R., Psomas, A., Puhlmann, H., Thimonier, A., Waldner, P., Zimmermann, S., & Walthert, L. (2022). Soil–plant interactions modulated water availability of Swiss forests during the 2015 and 2018 droughts. *Global Change Biology*, 28(20), 5928–5944.
- Mildenhall, B., Srinivasan, P. P., Tancik, M., Barron, J. T., Ramamoorthi, R., & Ng, R. (2020). NeRF: Representing scenes as neural radiance fields for view synthesis. In *European Conference on Computer Vision (ECCV)* (pp. 405–421).
- Paini, A. (2019). The salience of woodland in the Dolomites (Italian Alps). In *Cultural models of nature*.
- Rogora, M., Frate, L., Carranza, M. L., Freppaz, M., Stanisci, A., Bertani, I., ... & Matteucci, G. (2018). Assessment of climate change effects on mountain ecosystems through a cross-site analysis in the Alps and Apennines. *Science of the Total Environment*, 624, 1429–1442.
- Rutzinger, M., Höfle, B., Lindenbergh, R., Oude Elberink, S., Pirotti, F., Sailer, R., Scaioni, M., Stötter, J., Wujanz, D., 2016. Close-Range Sensing Techniques in Alpine Terrain. *ISPRS Ann. Photogramm. Remote Sens. Spat. Inf. Sci.* III-6, 15-22.
- Rutzinger, M., Bremer, M., Höfle, B., Hämmerle, M., Lindenbergh, R., Oude Elberink, S., Pirotti, F., Scaioni, M., Wujanz, D., Zieher, T., 2018. Training in Innovative Technologies for Close-Range Sensing in Alpine Terrain. *ISPRS Ann. Photogramm. Remote Sens. Spat. Inf. Sci.* IV-2, 239-246.
- Rutzinger, M., Anders, K., Bremer, M., Höfle, B., Lindenbergh, R. C., Oude Elberink, S., ... & Zieher, T. (2020). Training in innovative technologies for Close-range Sensing in Alpine terrain. In *XXIVth ISPRS Congress 2020* (pp. 243-250). International Society for Photogrammetry and Remote Sensing (ISPRS).
- Schmidt-Walter, P., Trotsiuk, V., Meusbürger, K., Zacios, M., & Meesenburg, H. (2020). Advancing simulations of water fluxes, soil moisture and drought stress by using the LWF-Brook90 hydrological model in R. *Agricultural and Forest Meteorology*, 291, 108023.
- Tancik, M., Weber, E., Ng, E., Li, R., Yi, B., Wang, T., ... & Kanazawa, A. (2023). Nerfstudio: A modular framework for neural radiance field development. In *ACM SIGGRAPH 2023 Conference Proceedings* (pp. 1–12).
- Torres, R., Snoeij, P., Geudtner, D., Bibby, D., Davidson, M., Attema, E., Potin, P., Rommen, B., Floury, N., Brown, M., Traver, I. N., Deghaye, P., Duesmann, B., Rosich, B., Miranda, N., Bruno, C., L'Abbate, M., Croci, R., Pietropaolo, A., ... Rostan, F. (2012). GMES Sentinel-1 mission. *Remote Sensing of Environment*, 120, 9–24.
- Valle, E., Lamedica, S., Pilli, R., & Anfodillo, T. (2009). Land use change and forest carbon sink assessment in an Alpine mountain area of the Veneto Region (Northeast Italy). *Mountain Research and Development*, 29, 161–168.
- Vorobevskii, I., Luong, T. T., Kronenberg, R., & Petzold, R. (2024a). High-resolution operational soil moisture monitoring for forests in central Germany. *Hydrology and Earth System Sciences*, 28(15), 3567–3595.
- Vorobevskii, I., Luong, T. T., & Kronenberg, R. (2024b). Seasonal forecasting of local-scale soil moisture droughts with Global BROOK90: A case study of the European drought of 2018. *Natural Hazards and Earth System Sciences*, 24(2), 681–697.
- Vosselman, G., & Maas, H. G. (2010). *Airborne and terrestrial laser scanning*. Whittles Publishing.
- Wehr, A., & Lohr, U. (1999). Airborne laser scanning—an introduction and overview. *ISPRS Journal of Photogrammetry and Remote Sensing*, 54(2–3), 68–82.
- Westoby, M. J., Brasington, J., Glasser, N. F., Hambrey, M. J., & Reynolds, J. M. (2012). 'Structure-from-Motion' photogrammetry: A low-cost, effective tool for geoscience applications. *Geomorphology*, 179, 300–314.
- Xu, C., Kerr, J., & Kanazawa, A. (2024). Splatfacto-w: A Nerfstudio implementation of Gaussian splatting for unconstrained photo collections. *arXiv preprint arXiv:2407.12306*.